Journal of Materials Chemistry A

Accepted Manuscript

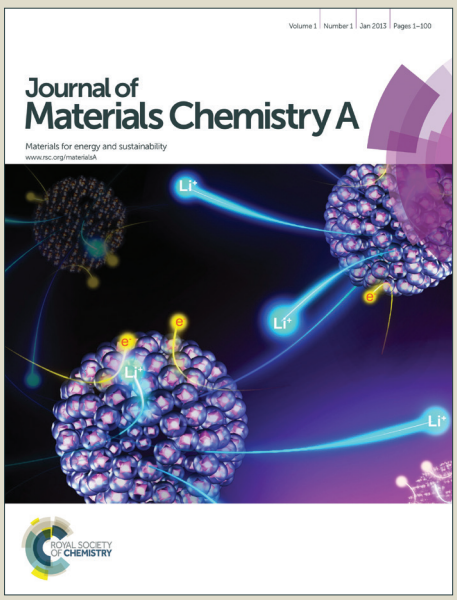

ROYAL SOCIETY OF CHEMISTRY

www.rsc.org/materialsA

Cite this: DOI: 10.1039/c0xx00000x

www.rsc.org/xxxxxx

COMMUNICATION

Three-Step Sequential Solution Deposition of PbI_2-Free $CH_3NH_3PbI_3$ Perovskite

Yixin Zhao[a*] and Kai Zhu[b*]

Received (in XXX, XXX) Xth XXXXXXXXX 20XX, Accepted Xth XXXXXXXXX 20XX

DOI: 10.1039/b000000x

We demonstrate a three-step sequential solution process to prepare PbI_2-free $CH_3NH_3PbI_3$ perovskite films. In this three-step method, a thermally unstable stoichiometric $PbI_2 \cdot CH_3NH_3Cl$ precursor film is first deposited on the mesoporous TiO_2 substrate, followed by thermal decomposition to form PbI_2, which is finally converted into $CH_3NH_3PbI_3$ by dipping in a regular isopropanol solution of CH_3NH_3I at room temperature. In comparison to the two-step approach using similar processing conditions, the three-step method enables the formation of PbI_2 film through the thermal decomposition of the $PbI_2 \cdot CH_3NH_3Cl$ precursor film. This facilitates a rapid conversion of PbI_2 to $CH_3NH_3PbI_3$ without any traceable residue PbI_2 in the final conversion step, leading to an improved device performance.

Introduction

Organometallic halide perovskites have become a promising class of light absorbers for low-cost, high-efficiency solar cells. The efficiency of perovskite solar cells has increased to 17.9% from an initial 3.8% within 5 years.[1-7] Perovskite deposition in most literature reports is by solution chemistry, mainly following two synthesis routes. The first approach is a one-step solution process via spin coating of the perovskite precursor onto the substrate, followed by thermal annealing to crystallize the perovskite film.[8-14] The second commonly used synthetic approach is a two-step sequential solution deposition.[4, 15-17] Two-step sequential deposition of lead halide perovskite was initially reported by Mitzi *et al.* in the 1990s.[18] It was recently adapted by Grätzel and co-workers to fabricate lead halide perovskite solar cells.[4] It has since become a popular method for growing perovskite films.[4] In a typical two-step sequential solution synthesis of perovskite such as $CH_3NH_3PbI_3$ (or $MAPbI_3$), PbI_2 is first deposited onto the substrate (mesoporous or planar scaffold) from a dimethylformamide (DMF) solution, followed by a conversion reaction to form $MAPbI_3$ by dipping the PbI_2 film in an anhydrous isopropanol (IPA) solution of CH_3NH_3I (or MAI), before final drying at elevated temperature (e.g., 100°C).

One advantage of the two-step method over the regular one-step method is that the deposited perovskite film is compact and uniform, leading to the demonstration of high-performance solar cells.[19-23] For the two-step method, the growth and film morphology of the final perovskite $MAPbI_3$ depend strongly on the initial PbI_2 film deposition during the first step of the process. Because PbI_2 tends to form a flat, layered structure, a compact and uniform PbI_2 film is usually formed. One of the challenges for the two-step deposition is to convert PbI_2 to perovskites. It is generally perceived that a high-quality perovskite needs a dense layer of PbI_2 precursor film; but a dense crystalline PbI_2 film is generally more difficult to convert completely into perovskite. In order to obtain a full conversion of PbI_2 to $MAPbI_3$, Mitzi and his coworkers had to soak the PbI_2 film in MAI isopropanol solution for hours.[18] This long reaction time in MAI solution could lead to the dissolution (sometimes peeling off) of perovskites. Also, the water content (or moisture) in regular IPA or accumulated overtime for anhydrous IPA could accelerate the degradation process, when the dipping/reaction time is long. Several strategies have been developed to address this challenge, including using elevated reaction temperature, controlling the crystallinity of the initial PbI_2 film, or using MAI vapor instead of MAI IPA solution.[15, 24, 25] These approaches have shown certain improvement to the PbI_2-to-perovskite conversion without causing significant degradation of the $MAPbI_3$ film during the conversion reaction process.

In this report, we demonstrate a new three-step sequential deposition method for preparing PbI_2-free $MAPbI_3$ films. Using a regular two-step approach, we find it difficult to completely convert PbI_2 into $MAPbI_3$ without causing significant degradation of the perovskite film. In contrast, by using the three-step sequential solution deposition approach, where a thermally unstable stoichiometric $PbI_2 \cdot CH_3NH_3Cl$ ($PbI_2 \cdot MACl$) precursor film is first deposited on the mesoporous TiO_2 substrate and followed by thermal decomposition to form PbI_2, the PbI_2 film can be rapidly converted into $MAPbI_3$ without any PbI_2 residue by using the regular MAI IPA solution at room temperature, leading to improved device performance.

Experimental

Materials. The MAI and MACl were synthesized by reacting methylamine (MA) with HI and HCl, respectively, followed by purification as previously reported.[10, 14] A patterned fluorine-doped tin oxide (FTO) was first deposited with a blocking layer by spray pyrolysis at 450 °C using 0.2 M Ti(IV) bis(ethyl acetoacetate)-diisopropoxide 1-butanol solution, followed by 450 °C annealing in air for one hour. A 500-nm-thick mesoporous

TiO_2 film was then screen coated onto FTO followed by 500° C annealing in air for 30 min, as detailed previously.[26] The TiO_2 film was then treated in 40 mM $TiCl_4$ aqueous solution at 65° C for 30 min. These $TiCl_4$-treated TiO_2 films were then sequentially rinsed by deionized (DI) water, blown dry in air, and finally annealed at 500° C for 30 min.

Two-step deposition of perovskites. 0.4–1.0 M PbI_2 (99.99%) DMF solution was spin coated onto the mesoporous TiO_2 film at 3000 rpm for 20 s. The deposited PbI_2 film was then annealed at 70° C for 5 min. The PbI_2 film was cooled to room temperature and then immersed into a 10 mg MAI/mL IPA solution for different times (2–60 min), followed by being rinsed with IPA, blown dry with N_2, and then annealed at 70° C for 5 min. The IPA used in this report is the regular ACS Reagent, ≥99.5% grade.

Three-step deposition of perovskites. A DMF precursor solution of 1.0 M equal molar ratio PbI_2 and MACl was first spin coated onto the mesoporous TiO_2 film at 3000 rpm for 20 s. The deposited film was then annealed at 130 ° C for 30 min to decompose to a yellow PbI_2 film, followed by cooling to room temperature. The yellow PbI_2 film was then immersed into a 10 mg MAI/mL IPA solution for 30 s, followed by being rinsed with IPA, blown dry by N_2, and then annealed at 70° C for 5 min.

Device preparation. The perovskite-deposited electrodes were first coated with a layer of hole transport material (HTM) by spin coating at 4000 rpm for 20 s using 0.1 M spiro-MeOTAD, 0.035 M bis(trifluoromethane)sulfonimide lithium salt (Li-TFSi), and 0.12 M 4-*tert*-butylpyridine (tBP) in chlorobenzene/acetonitrile (10:1, v/v) solution. Finally, a 150-nm-thick Ag contact layer was deposited by thermal evaporation, as previously described.[27]

Characterization. The crystal structures of the perovskite films were measured by X-ray diffraction (XRD, Bruker D8 ADVANCE with Cu Kα radiation). The absorption spectra of the planar perovskite films were characterized by an ultraviolet-visible (UV-vis) spectrophotometer (Cary-60). J–V curves were measured with a Keithley 2400 source meter under simulated AM 1.5G illumination (100 mW/cm^2; Oriel Sol3A Class AAA Solar Simulator) with a scan rate of about 0.1 V/s. A typical cell area was about 0.16 cm^2 as defined by a shadow mask.

Result and discussion

In the standard two-step method,[4] a 1.0 M PbI_2 precursor solution is normally used to obtain sufficient deposition of $MAPbI_3$ to absorb light. We examined the time evolution of the conversion of PbI_2 into $MAPbI_3$ by using UV-vis and XRD measurements. Figure 1a shows the effect of MAI dipping time on changes of the XRD patterns. When the PbI_2 film is dipped in MAI for 2 min, there is an incomplete conversion as evidenced by the existence of both the PbI_2 (near 12.6°) and $MAPbI_3$ (near 14°) diffraction peaks with similar peak intensities. The intensity of the $MAPbI_3$ peak increases, whereas the PbI_2 peak intensity decreases with longer MAI dipping time (10–60 min). Even with a 60-min dipping time, there is still a noticeable amount of PbI_2 in the film as indicated by the characteristic PbI_2 diffraction peak. However, the intensity of the PbI_2 peak is much smaller and almost negligible compared to the $MAPbI_3$ peak when the dipping time is more than 30 min.

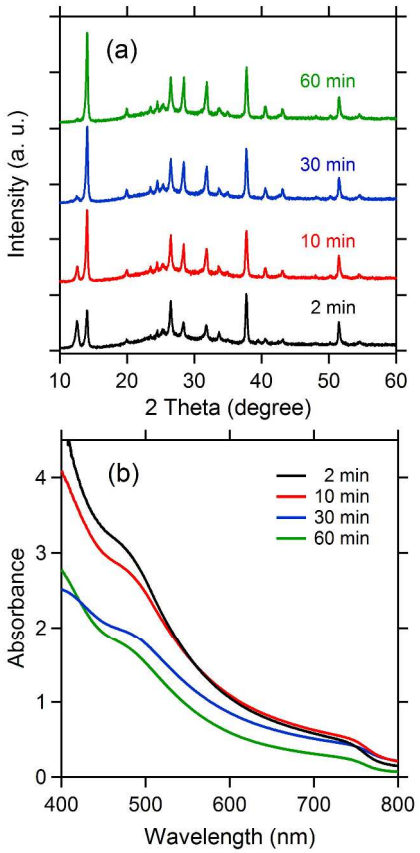

Fig. 1 Effect of the dipping time in the 10 mg MAI/mL IPA solution on the evolution of (a) XRD patterns and (b) UV-vis absorption spectra for the perovskite films deposited from 1.0 M PbI_2 precursor on mesoporous TiO_2 film.

Table 1 Effect of the MAI dipping time on the perovskite solar cell photovoltaic parameters: short-circuit photocurrent density, J_{sc}; open-circuit voltage, V_{oc}; fill factor, FF; and conversion efficiency, η.

Dipping Time [min]	J_{sc} [mA/cm^2]	V_{oc} [V]	FF	η [%]
2	8.58	0.859	0.346	2.55
10	11.41	0.837	0.403	3.85
30	14.84	0.899	0.431	5.75
60	11.07	0.911	0.455	4.59

During the conversion process in the second step, the initial yellow PbI_2 film slowly changes color to brown or dark brown depending on the dipping time in the MAI solution. Figure 1b shows the UV-vis absorption spectra of the resulting films as a function of the dipping/conversion time. Although the XRD measurement indicates a significant fraction of PbI_2 for the 2-min dipped sample, the UV-vis spectrum of this sample shows a typical $MAPbI_3$ absorbance as shown in Figure 1b. The direct absorbance by the residue PbI_2 is likely hidden by the absorption spectrum from the partially converted $MAPbI_3$ within the film. Because the regular IPA solution can dissolve $MAPbI_3$, longer dipping time eventually leads to a significant drop of absorption across the entire wavelength range, despite more conversion of

PbI_2 to $MAPbI_3$, as suggested by the XRD result. As a result, the 60-min dipped sample only display about half the absorbance compared to the 2-min dipped sample. It is worth noting that because of this issue, a recent study uses a vapour-assisted two-step approach to avoid the partial dissolution of $MAPbI_3$ in the IPA solution.[25]

The impact of the MAI dipping time on the photovoltaic parameters of the perovskite solar cells are compared in Table 1. When the dipping time is increased from 2 to 60 min, the short-circuit photocurrent density first increases and then decreases, with a peak value (14.84 mA/cm^2) reached at 30 min, which reflects the balance between perovskite conversion and dissolution during the second process step, as shown in Figure 1. Fill factor of these devices increases significantly with the increase of dipping time, from 0.346 at 2 min to 0.455 at 60 min. The overall conversion efficiency essentially follows the trend of photocurrent, increasing from 2.55% at 2 min to 5.75% at 30 min, and then decreases to 4.59% at 60 min. These results indicate that it is important to have more complete conversion of PbI_2 to $MAPbI_3$ without significant dissolution of $MAPbI_3$ in order to reach reasonable device performance. We have previously examined the role of PbI_2 in mesoporous perovskite solar cells. We found that the PbI_2-based solar cell has about a factor of five slower transport rate than perovskite solar cells.[28] Thus, it is critical to develop certain techniques to minimize the amount of

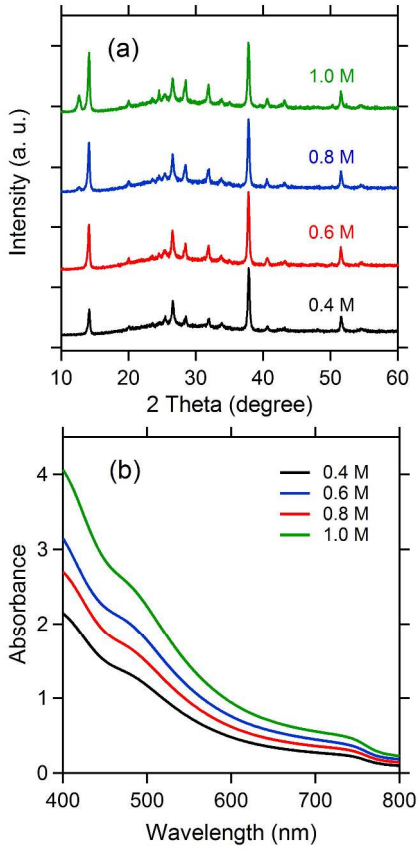

Fig. 2 Effect of PbI_2 concentration (0.4–1.0 M) on the (a) XRD patterns and (b) UV-vis absorption spectra of the perovskite films deposited on mesoporous TiO_2 film after dipping in 10 mg MAI/mL IPA solution for 10 min.

Table 2. Effect of PbI_2 concentration (0.4–1.0 M) on the perovskite solar cell photovoltaic parameters. The second-step MAI dipping time is 10 min for all samples.

Concentration [M]	J_{sc} [mA/cm^2]	Voc [V]	FF	η [%]
0.4	10.27	0.842	0.609	5.27
0.6	14.79	0.836	0.585	7.23
0.8	11.73	0.830	0.55	5.35
1.0	11.40	0.837	0.403	3.85

PbI_2 for two-step deposition.

A recent study has demonstrated a complete conversion of PbI_2 to $MAPbI_3$ by using a lower concentration (e.g., 0.4 M) of PbI_2 precursor solution.[29] Here, we compare the impact of varying PbI_2 concentration on the PbI_2-to-$MAPbI_3$ conversion using the two-step method. The concentration of the PbI_2 precursor solution was changed from 0.4 to 1.0 M. To avoid the dissolution of $MAPbI_3$ in the IPA solution, the dipping duration of PbI_2 film in the MAI IPA solution was fixed at 10 min for all samples. Figure 2a shows the XRD measurements of the perovskite films using different PbI_2 concentration with 10-min dipping time during the second process step. The intensity of the characteristic PbI_2 diffraction peak decreases significantly when the PbI_2 concentration is reduced from 1.0 to 0.8 M. The PbI_2 peak disappears from the diffraction pattern when the PbI_2 concentration is further reduced to 0.6 and 0.4 M, suggesting a complete conversion of PbI_2 to $MAPbI_3$ using a low-concentration PbI_2 precursor with 10-min dipping in the MAI IPA solution. We speculate that the lower concentration PbI_2 precursor solutions (e.g., 0.4–0.6 M) lead to less infiltration of PbI_2 in the mesoporous TiO_2 films than the higher concentration ones (e.g., 0.8–1.0 M PbI_2). A lower degree of pore filing of PbI_2 can promote the conversion of PbI_2 into $MAPbI_3$ by facilitating the intercalation of MAI into PbI_2; but it also results in lower absorbance due to less $MAPbI_3$ deposition. Figure 2b compares the effect of PbI_2 concentration on the UV-vis absorption spectra of the perovskite films. A higher PbI_2 concentration generally leads to stronger absorbance. The perovskite film based on a 0.4 M PbI_2 precursor displays only about half the absorbance of the perovskite film based on a 1.0 M PbI_2 precursor.

Table 2 shows the photovoltaic parameters (J_{sc}, V_{oc}, FF and η) of the solar cells based on the $MAPbI_3$ films prepared using different concentrations of PbI_2 precursor solutions with 10-min dipping in the MAI solution during the second process step. The 0.8-M sample exhibits a low photocurrent density similar to the 1.0-M sample, which can be attributed to the residue PbI_2 observed from XRD. In contrast, the 0.6-M sample without any PbI_2 residue exhibits a reasonable photocurrent density despite its lower absorption than the 1.0-M sample (Figure 1b). However, the lowest J_{sc} value was observed for the 0.4-M sample, for which the poor light absorption clearly limits the device performance. As a balance for optimizing both the light absorption and conversion of PbI_2 to $MAPbI_3$, the best device performance efficiency was obtained for the 0.6-M sample with a cell efficiency of about 7.23%. Thus, it appears that the regular isopropanol may not be suitable for the standard two-step method because of the $MAPbI_3$ dissolution issue (as discussed above) and

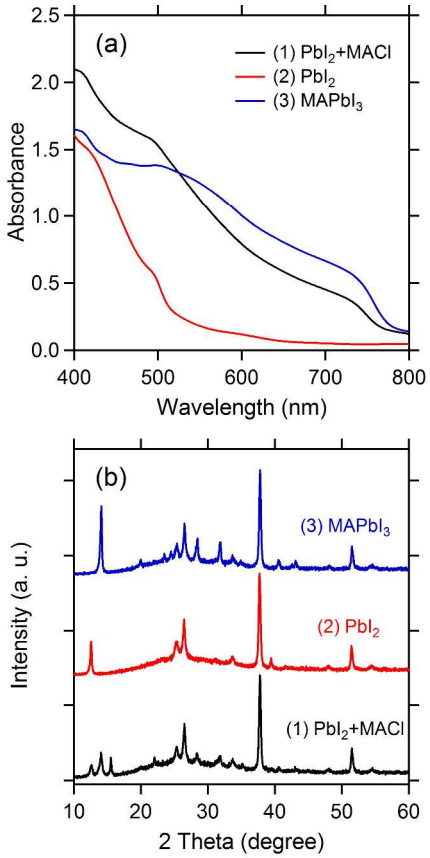

Fig. 3 (a) UV-vis absorption spectra and (b) XRD patterns of the films in each of the three steps: (1) initial film formation from precursor of mixed PbI_2 and MACl; (2) thermally decomposed PbI_2 film from the second step; (3) final $MAPbI_3$ formed after dipping in MAI solution after the third step.

the difficulty of getting a PbI_2-free $MAPbI_3$ film with sufficient absorption. It is worth emphasizing again that this challenge is caused mainly by the difficulty associated with MAI intercalation into a higher pore-filling PbI_2 film during the final (second) reaction step.

To address the abovementioned challenge for two-step deposition, we examined a new three-step sequential deposition method. In the three-step method, a precursor of mixed PbI_2 and MACl (with equal molar concentration) is first deposited onto the mesoporous TiO_2 film. The obtained precursor film when annealed at 130°C for 1 min exhibits a light brown color with an unknown XRD pattern. Its XRD pattern and UV-vis absorption spectra are shown in Figure 3a and 3b, respectively, as indicated as step (1) in the figure. The absorption spectra are similar to those of $MAPbI_3$; however, their XRD patterns are very different. This unknown compound (denoted as PbI_2+MACl) is likely a mixture of $MAPbCl_3$, $MAPbI_3$, and some unknown structure.[30] When annealed at 130°C in air, the brown film slowly turns to a yellow color. After annealing at 130°C for 30 min, the PbI_2+MACl film is thermally decomposed to PbI_2, as suggested by its UV-vis spectra and XRD pattern (Figure 3, step 2). No traceable Cl content can be found in this film by the energy dispersive X-ray (EDX) analysis. The Pb:I ratio is about 1:2.1±0.3 with a complete loss of Cl (within the EDX detection

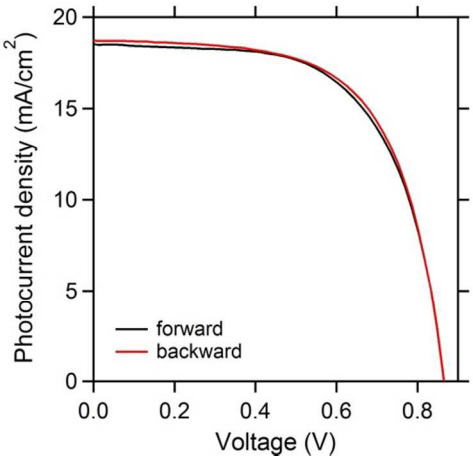

Fig. 4 J–V characteristic of a perovskite solar cell based on the $MAPbI_3$ film prepared from the three-step approach.

limit of ~1%). This observation is consistent with our previous studies on the sublimation of MACl with thermal annealing.[14, 27]

The PbI_2 film formed from thermal decomposition during the second process step turns to dark brown almost immediately after dipping in MAI solution (with regular IPA) during the third (conversion) step. It takes only about 30 s for the yellow PbI_2 film to convert into a dark-brown $MAPbI_3$ film (Figure 3a, step 3) without any traceable PbI_2 from its XRD pattern (Figure 3b, step 3). The $MAPbI_3$ prepared from the initial 1.0 M PbI_2·MACl precursor by the three-step method exhibits a strong absorption (especially in the long-wavelength region) that is similar to the film prepared from the regular two-step approach using a 1.0 M PbI_2 precursor. Figure 4 shows the typical J–V characteristics of a perovskite solar cell using the three-step deposition method. The cell efficiency is about 10.11%, with a J_{sc} of 18.64 mA/cm^2, V_{oc} of 0.868 V, and FF of 0.625. Both forward and backward J–V scans are shown in Figure 4. The hysteresis is about 1%, and thus, can be considered negligible.

The above results demonstrate that the three-step method provides a promising way to address the challenge associated with the PbI_2 conversion for the regular two-step method. Here, we hypothesis that the quick PbI_2-to-$MAPbI_3$ conversion kinetics observed results from the higher exposed surface of the PbI_2 film prepared through the second step (thermal decomposition process) in the three-step deposition method. Our previous study has indicated that MACl sublimation could introduce some pores in the film.[27] The formation of pores resulting from the release of MACl in the thermal decomposition step is expected to form a PbI_2 film with a more porous structure than the relatively compact PbI_2 film deposited directly from the PbI_2 precursor. The larger exposed surface of the porous PbI_2 film would enable a faster intercalation reaction of MAI with PbI_2 during the final conversion step, leading to a complete conversion of PbI_2 within 30 s. With such a short dipping time, the issue of $MAPbI_3$ dissolution in the IPA solution is effectively mitigated.

Conclusions

We investigated the effect of varying PbI_2 concentration (during the first step) and changing the dipping time in MAI

solution (during the second step) using the two-step sequential deposition on the optical/structural properties of perovskite films and their relationship to the device characteristics of solar cells based on these perovskite films. We find that for the high-concentration (1.0 M) PbI_2 precursor, the conversion of PbI_2 to $MAPbI_3$ requires a long conversion time in the MAI IPA solution. The long exposure to IPA solution causes the dissolution of the converted $MAPbI_3$ film, leading to reduced photocurrent generation, and consequently, poor device performance. On the other hand, a short exposure of PbI_2 to the MAI IPA solution results in a partial conversion of the film with significant PbI_2 residue, which also limits the device performance. Using a less concentrated PbI_2 solution (e.g., 0.4 M) shows complete conversion of PbI_2 with fixed reaction duration (10 min). However, the poorer light absorption for the perovskite film prepared with a low concentration of PbI_2 also limits the device performance. To address this dilemma, we demonstrate a new three-step solution process to prepare $MAPbI_3$ perovskite by using a MAI solution with regular (non-anhydrous) IPA. In comparison to the two-step approach using similar processing conditions, the three-step method enables the formation of PbI_2 film through the thermal decomposition of the PbI_2+MACl precursor film. This facilitates a rapid conversion of PbI_2 to $MAPbI_3$ without any traceable residue PbI_2 in the final conversion step, leading to improved device performance. Thus, our reported three-step solution deposition using regular IPA represents a promising alternative deposition method for preparing low-cost, high-efficiency perovskite solar cells.

Acknowledgement

YZ is thankful for the support of the NSFC (Grant 51372151 and 21303103). KZ acknowledges the support by the U.S. Department of Energy/National Renewable Energy Laboratory's Laboratory Directed Research and Development (LDRD) program under Contract No. DE-AC36-08GO28308.

Notes and references

[a] *School of Environmental Science and Engineering, Shanghai Jiao Tong University, 800 Dongchuan Rd., Shanghai 200240, China E-mail: yixin.zhao@sjtu.edu.cn*
[b] *Chemical and Materials Science Center, National Renewable Energy Laboratory, 15013 Denver West Parkway, Golden, CO 8040.1, USA E-mail: kai.zhu@nrel.gov*

1. A. Kojima, K. Teshima, Y. Shirai and T. Miyasaka, *J. Am. Chem. Soc.*, 2009, **131**, 6050-6051.
2. J.-H. Im, C.-R. Lee, J.-W. Lee, S.-W. Park and N.-G. Park, *Nanoscale*, 2011, **3**, 4088-4093.
3. N. J. Jeon, J. H. Noh, Y. C. Kim, W. S. Yang, S. Ryu and S. I. Seok, *Nat. Mater.*, 2014, **13**, 897–903.
4. J. Burschka, N. Pellet, S. J. Moon, R. Humphry-Baker, P. Gao, M. K. Nazeeruddin and M. Gratzel, *Nature*, 2013, **499**, 316-319.
5. M. M. Lee, J. Teuscher, T. Miyasaka, T. N. Murakami and H. J. Snaith, *Science*, 2012, **338**, 643-647.
6. R. F. Service, *Science*, 2014, **344**, 458.
7. H.-S. Kim, C.-R. Lee, J.-H. Im, K.-B. Lee, T. Moehl, A. Marchioro, S.-J. Moon, R. Humphry-Baker, J.-H. Yum, J. E. Moser, M. Gratzel and N.-G. Park, *Sci. Rep.*, 2012, **2**, 1-7.
8. B. Conings, L. Baeten, C. De Dobbelaere, J. D'Haen, J. Manca and H.-G. Boyen, *Adv. Mater.*, 2014, **26**, 2041-2046.
9. P.-W. Liang, C.-Y. Liao, C.-C. Chueh, F. Zuo, S. T. Williams, X.-K. Xin, J. Lin and A. K. Y. Jen, *Adv. Mater.*, 2014, **26**, 3748-3754.
10. Y. Zhao and K. Zhu, *J. Phys. Chem. Lett.*, 2013, **4**, 2880-2884.
11. J. T. Wang, J. M. Ball, E. M. Barea, A. Abate, J. A. Alexander-Webber, J. Huang, M. Saliba, I. Mora-Sero, J. Bisquert, H. J. Snaith and R. J. Nicolas, *Nano Lett.*, 2013, **14**, 724-730.
12. H.-S. Kim, J.-W. Lee, N. Yantara, P. P. Boix, S. A. Kulkarni, S. Mhaisalkar, M. Grätzel and N.-G. Park, *Nano Lett.*, 2013, **13**, 2412-2417.
13. J. H. Noh, S. H. Im, J. H. Heo, T. N. Mandal and S. I. Seok, *Nano Lett.*, 2013, **13**, 1764-1769.
14. Y. Zhao and K. Zhu, *J. Phys. Chem. C*, 2014, **118**, 9412–9418.
15. P. Docampo, F. Hanusch, S. D. Stranks, M. Döblinger, J. M. Feckl, M. Ehrensperger, N. K. Minar, M. B. Johnston, H. J. Snaith and T. Bein, *Adv. Energy Mater.*, 2014, DOI: 10.1002/aenm.201400355.
16. A. Yella, L.-P. Heiniger, P. Gao, M. K. Nazeeruddin and M. Grätzel, *Nano Lett.*, 2014, **14**, 2591-2596.
17. D. Liu and T. L. Kelly, *Nat. Photon.*, 2014, **8**, 133-138.
18. K. Liang, D. B. Mitzi and M. T. Prikas, *Chem. Mater.*, 1998, **10**, 403-411.
19. N. Pellet, P. Gao, G. Gregori, T.-Y. Yang, M. K. Nazeeruddin, J. Maier and M. Grätzel, *Angew. Chem. Int. Ed.*, 2014, **53**, 3151-3157.
20. J. J. Shi, J. Dong, S. T. Lv, Y. Z. Xu, L. F. Zhu, J. Y. Xiao, X. Xu, H. J. Wu, D. M. Li, Y. H. Luo and Q. B. Meng, *Appl. Phys. Lett.*, 2014, **104**, 063901.
21. H.-S. Kim, S. H. Im and N.-G. Park, *J. Phys. Chem. C*, 2014, **118**, 5615-5625.
22. P. Qin, S. Tanaka, S. Ito, N. Tetreault, K. Manabe, H. Nishino, M. K. Nazeeruddin and M. Grätzel, *Nat. Commun.*, 2014, **5**, 3834.
23. M. A. Green, A. Ho-Baillie and H. J. Snaith, *Nat. Photon.*, 2014, **8**, 506-514.
24. Y. Wu, A. Islam, X. Yang, C. Qin, J. Liu, K. Zhang, W. Peng and L. Han, *Energy Environ. Sci.*, 2014, **7**, 2934-2938.
25. Q. Chen, H. Zhou, Z. Hong, S. Luo, H.-S. Duan, H.-H. Wang, Y. Liu, G. Li and Y. Yang, *J. Am. Chem. Soc.*, 2014, **136**, 622-625.
26. Y. Zhao, A. M. Nardes and K. Zhu, *J. Phys. Chem. Lett.*, 2014, **5**, 490-494.
27. Y. Zhao and K. Zhu, *J. Am. Chem. Soc.*, 2014, **136**, 12241-12244.
28. Y. Zhao, A. Nardes and K. Zhu, *Faraday Discuss.*, 2014, DOI: 10.1039/C1034FD00128A.
29. D. Bi, S.-J. Moon, L. Haggman, G. Boschloo, L. Yang, E. M. J. Johansson, M. K. Nazeeruddin, M. Gratzel and A. Hagfeldt, *RSC Adv.*, 2013, **3**, 18762-18766.
30. B.-W. Park, B. Philippe, T. Gustafsson, K. Sveinbjörnsson, A. Hagfeldt, E. M. J. Johansson and G. Boschloo, *Chem. Mater.*, 2014, **26**, 4466-4471.

Table of Contents Entry

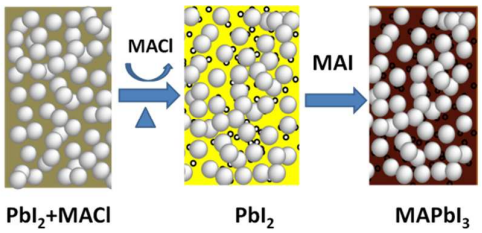

We demonstrate a facile approach of preparing PbI_2-free $CH_3NH_3PbI_3$ perovskite films via a three-step sequential solution process.